Supporting Information

Isotopic-Perturbation NMR Study of Hydrogen-Bond Symmetry in Solution: Temperature Dependence and Comparison of OHO and ODO Hydrogen Bonds

Charles L. Perrin,* Annadka Shrinidhi, and Kathryn D. Burke[a]

Department of Chemistry and Biochemistry, University of California—San Diego, La Jolla, CA 92093-0358, United States

*Corresponding author: cperrin@ucsd.edu

[a]Current address: Department of Chemistry and Biochemistry, University of Delaware, Newark, DE 19716, USA

Experimental

Materials. Labelled reagents, including water-^{18}O ($H_2{}^{18}O$, 1-mL ampules, 97% ^{18}O), water-d_2 (D_2O, 99.9% D), $CDCl_3$, and acetonitrile-d_3 (CD_3CN, 99% D), were obtained from Cambridge Isotope Laboratories, Inc. and used without additional purification. Milli-Q water was used for syntheses and for sample preparation, as required. Tetrahydrofuran (THF, Aldrich, >99.9% anhydrous) and tetrabutylammonium cyanide (Aldrich, 95%) were used without additional purification. Tetrabutylammonium hydroxide (Aldrich, 40 wt% in water) was standardized by titration with 1.000 ± 0.005 M HCl. Pentafluorophenol (Oakwood, 98%) and peracetic acid (Acros, 35% in glacial acetic acid) were used without additional purification.

4,5,6,7-Tetrahydro-1,3-isobenzofurandione (3,4,5,6-tetrahydrophthalic anhydride, Aldrich) was recrystallized from diethyl ether (mp 69–75°C, lit[1] 74°C). Sodium hydroxide-^{18}O (~97% ^{18}O) powder was readily prepared by careful addition of metallic sodium (50 mg, Aldrich) to $H_2{}^{18}O$ (500 μL) at 0°C with stirring, followed by drying under high vacuum.

Instrumentation

Mass spectral data were obtained on a Thermo LCQ deca-MS spectrometer using ESI-MS in a negative-ion mode. ^{13}C NMR spectra were obtained on a JEOL ECA500 FT-NMR spectrometer (500.2 MHz ^{1}H, 125.8 MHz ^{13}C), with $CDCl_3/CHCl_3$ as internal standard. ^{19}F NMR spectra (282 MHz) were obtained on a Bruker AVA300 FT-NMR spectrometer with sodium tetrafluoroborate ($NaBF_4$, s, -151.04 ppm and q, -151.10 ppm)[2] or hexafluorobenzene (C_6F_6, s, -163.00 ppm)[3] as internal standards in aqueous or organic solvents, respectively. ^{1}H NMR spectra (300 MHz) were obtained with 3-(trimethylsilyl)-1-propanesulfonic acid-d_6 (DSS, 0 ppm) or tetramethylsilane (TMS, 0 ppm) as internal standards in aqueous solutions or organic solvents, respectively.

^{1}H NMR spectra were collected with a window of 13.8 KHz (0-22 ppm) to include any deshielded OHO signal. Reasonable spectra were obtained with four transients and 16K points.

^{13}C NMR spectra were obtained using a heteronuclear broadband probe with ^{1}H decoupling centered at 2 ppm. The probe was tuned to the sample prior to gradient shimming. A spectral window of 8000 Hz (125 ppm to 185 ppm) was used with 32K data points and zero-filled to a final resolution of 64 points/Hz. Spectra were collected with 64 transients. Line broadening of 1.0 Hz was applied. ^{1}H and ^{13}C NMR acquisitions were obtained at temperatures from −60°C to 20°C.

^{19}F NMR spectra were obtained with sixteen transients, and a spectral window with 1.4 kHz (-124 to -129 ppm) was used with 32K data points, zero-filled to 128 points/Hz. Resolution was preserved by applying line broadening of only 0.1 Hz. Additionally, phase and baseline were corrected for any observed distortions. For each temperature the probe was set to the desired temperature and allowed to equilibrate for 10 minutes before spectra were obtained. The sample was shimmed at each temperature.

Spectra were processed using Bruker TopSpin 4.0, Academic Edition or ACD/NMR Processor Academic Edition.

NMR Sample Preparation and NMR Spectra

NMR samples were prepared as 0.3 M Bu_4N^+ **1**-*d*-$^{18}O_n$ in $CDCl_3$ and as 25-mM solutions of Bu_4N^+ **2**-*h*-$^{18}O_n$ or Bu_4N^+ **2**-*d*-$^{18}O_n$ in D_2O or CD_3CN. Samples were deoxygenated using the freeze-pump-thaw method and used without further drying, as no water impurity was detected by

^{1}H NMR. Prior to obtaining ^{13}C NMR data at each temperature, a ^{1}H NMR spectrum was obtained. ^{19}F chemical shifts were evaluated by placing the cursor at the center of each peak.

Synthesis and Characterization

Syntheses of Bu_4N^+ 3,4,5,6-tetrahydrophthalate-$^{18}O_{0–4}$ (**1**-*h*-$^{18}O_n$) and Bu_4N^+ 3,4,5,6-tetrahydrophthalate-*d* -$^{18}O_{0–4}$ (**1**-*d*-$^{18}O_n$)

A mixture of ^{18}O isotopologues of 3,4,5,6-tetrahydrophthalic diacid was synthesized by combining 20-30 mg (0.1-0.2 mmol) of the anhydride with 20.0 μL $H_2{}^{18}O$ and 50–70 μL anhydrous THF (to increase solubility) in a 3-mL conical reaction vessel equipped with a spin vane. The reaction mixture was stirred at room temperature for 1–6 days. Increasing incorporation of ^{18}O was confirmed by mass spectrometry. Bu_4N^+ OH^- (1 equivalent based on anhydride) was then added to the reaction vessel, and the solid Bu_4N^+ 3,4,5,6-tetrahydrophthalate-$^{18}O_{0–4}$ was isolated by removing the solvent in vacuo. Alternatively, D_2O (500 μL) was added to the hydrolysis mixture and the solution was stirred briefly before the addition of 1 equivalent (based on anhydride) of Bu_4N^+ OH^-. The solid Bu_4N^+ 3,4,5,6-tetrahydrophthalate-*d*-$^{18}O_{0–4}$ was then isolated by removing the solvent in vacuo. No further purification was performed. The D:H ratio was evaluated as 14:1 from the ratio of the integrals of the two broad singlets at ~20 ppm in the −50°C ^{1}H NMR spectra of **1**-*d* and **1**-*h*. ^{1}H NMR (500.2 MHz) $CDCl_3$: δ 3.2 (m, 8H), 2.4 (m, H_b, 4H), 1.5 (m, 8H), 1.5 (m, H_a, 4H), 1.3 (m, 8H), 0.9 (t, 12H, J = 7.2 Hz). ^{13}C NMR (125.8 MHz) $CDCl_3$: δ 171.3, 139.3, 58.7, 29.4, 23.9, 22.3, 19.7, 13.6 ppm.

Negative-ion mass spectrometry of ^{18}O-labeled **1** ($[M-H]^-$ = 169 m/z for $C_8H_9O_4^-$) was used to measure the relative amounts of ^{18}O-labeled isotopologues (Table S1). These values were corrected for ^{13}C content. Although each preparation produced slightly different ratios, all were very similar, and the ratios described here are representative.

Table S1. Masses and relative amounts of $^{18}O_{0–4}$ isotopologues of diacid **1**.

Mass (m/z)	$n(^{18}O)$	$P(n)$
169.19	0	0.244
171.14	1	0.498
173.13	2	0.222
175.22	3	0.030
177.10	4	0.006

Figure S1 shows the ^{1}H NMR spectrum for a mixture of ^{18}O-labeled isotopologues of **1**-*d* at −50°C. The peaks representing H_a and H_b appear 0.95 ppm apart from each other. This is highly indicative of monoanion **1**, because the diacid, the dianion (in water), and the anhydride starting material all have smaller peak separations. Although it has been replaced with a deuterium in this case, the acidic proton is highly deshielded and normally would appear near 20 ppm. At room temperature this peak is very broad and disappears into the baseline. However, at lower temperatures this peak begins to be visible, although it is still quite broad. A comparison of the integrations of **1**-*d* and **1**-*h* at −50°C was used to determine the D:H ratio of 14:1 (by comparing to a sample that was not washed with D_2O prior to monodeprotonation), suggesting that most protons in the H-bond have indeed been replaced by deuterons.

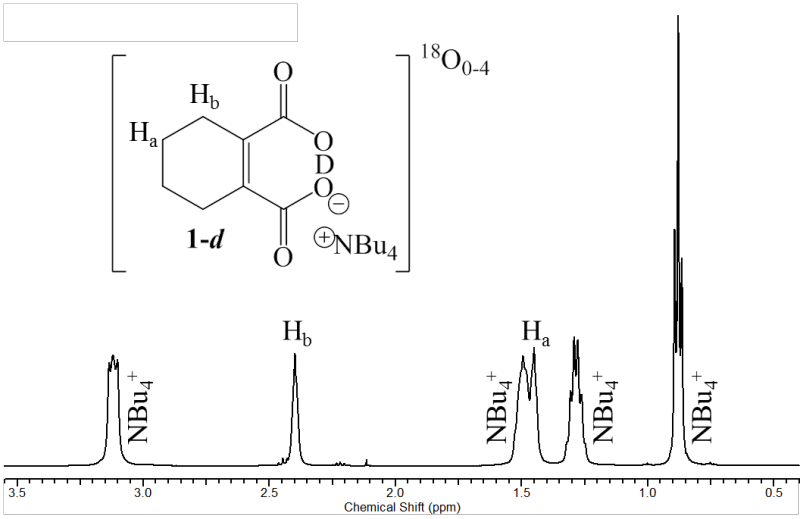

Figure S1. ^{1}H NMR spectrum of mixture of $^{18}O_{0–4}$-labeled isotopologues of Bu_4N^+ **1**-*d* in $CDCl_3$ at −50°C.

Table S2 lists the relative peak heights for $\mathbf{A_0}$ and $\mathbf{A_1}$ in Fig. 1 These intensities can also be estimated from the mass spectrometry data (Table S1), where $p(n)$, n = 0,1,2,3,4, represents the observed probability that **1**-*d* will be un-, mono-, di-, tri-, or tetra-labeled. These values are included in Table S2 and agree well with the relative peak heights, with a RMS deviation of 0.043.

Table S2. Relative peak heights of each ^{18}O-labeled carboxyl carbon in Fig. 1 and the distribution $P(n)$ from mass intensities in Table S1.

Signal	Relative Peak Height	$P(n)$
$\mathbf{A_0}$	0.573	0.530
$\mathbf{A_1}$	0.427	0.412
$\mathbf{A_2}$	--	0.058

Although there are six possible isotopologues of ^{18}O-labeled **1**-*d*, only three are major contributors in this sample, and the others will not be considered. Within each structure there are carboxyl carbons **A** and ipso carbons **B**. The ipso carbons will be considered later. The subscript for the carboxyl carbons represents the number of ^{18}Os bonded to that carbon. These structures ignore the conformational isotopomers for carboxyls with a single ^{18}O. These are analogous to RC(=^{16}O)OH and RC(=O)^{18}OH, for which the tautomeric equilibrium constant was estimated as 1.011.[4] Therefore although only one conformational isotopomer is shown for **1**-$^{18}O_1$ in Fig. 2, both are present, and in equal amounts. Furthermore, there are two isotopomers of **1**-$^{18}O_{2S}$, and the structure with both ^{18}Os attached to the same carbon is ignored because it is only half as populated as the one with ^{18}Os on opposite carbons.

The labeling depicted in Fig. 3 is supported by the mass spectrometry ratios in Table S1. These ratios can be separated into the contribution to each of the ipso carbon types listed in Fig. 2. $\mathbf{B_{01}}$ or $\mathbf{B_{10}}$ each represents half the monolabeled probability, $p(1)$, plus half the trilabeled probability, $p(4)$, and two-thirds of the dilabeled probability, $p(2)$. The two-thirds is because a second ^{18}O is twice as likely to be on the opposite carboxyl as on the already labeled carboxyl. The remaining one-third of $p(2)$ is split in half to represent $\mathbf{B_{02}}$ and $\mathbf{B_{20}}$. The contributions of the negligible amounts of dilabeled ($\mathbf{B_{02}}$ and $\mathbf{B_{20}}$), trilabeled, and tetralabeled compound can be

ignored when considering peak heights. The results of this analysis (Table S3) compare favorably with the relative peak heights associated with the peak assignments in Fig. 1 (RMS = 0.034). It should be noted that the $\mathbf{B_{02}}$ and $\mathbf{B_{20}}$ labels could be reversed (similarly for $\mathbf{B_{01}}$ and $\mathbf{B_{10}}$), but shielding patterns justify the assignment made herein.

Table S3. Relative peak heights of each ^{18}O-labeled carboxyl carbon in Fig. 1 and the binomial distribution $P(n)$ from mass intensities in Table S1.

Signal	Relative Peak Height	$P(n)$
$\mathbf{B_{02}}$	--	0.037
$\mathbf{B_{01}}$	0.313	0.264
$\mathbf{B_{00/11}}$	0.425	0.398
$\mathbf{B_{10}}$	0.262	0.264
$\mathbf{B_{20}}$	--	0.037

Synthesis of difluoromaleic Acid

Peracetic acid (35%, 109 mmol, 21 mL) was added into a 50-mL HDPE bottle and warmed to 60°C with stirring, followed by portionwise addition of pentafluorophenol (5 g, 27.2 mmol) over a period of 30 min. The reaction mixture was heated to 75°C and the stirring was continued. After 24 h the reaction mixture was acidified with hydrochloric acid (1*N*, 25 mL) and extracted with $CHCl_3$ (2 x 50 mL) to remove unreacted pentafluorophenol (2.5 g, 50%). The aqueous layer was evaporated to dryness in a rotary evaporator and the solid material thus obtained was sonicated in acetone (10 mL) for 1 min, filtered, and washed with acetone (2 x 10 mL. The undissolved residue was discarded. The collected acetone layers were dried with Na_2SO_4, the solvent was evaporated to dryness, and the solid obtained was recrystallized from CH_2Cl_2 to afford pure difluoromaleic acid (0.8 g, 39% based on unrecovered reactant, white solid, mp 219-220°C, lit.[5] 219-220°C). ^{1}H NMR (300 MHz, D_2O): no signals other than OH. ^{19}F NMR (282.3 MHz, D_2O): δ -126.3 (s, 2F) ppm. ESI-HRMS 150.9849, calculated for $C_4HF_2O_4^-$ $[M–H]^-$: 150.9848.

Synthesis of difluoromaleic anhydride

To a 25-mL round-bottomed flask fitted with a distillation apparatus, difluoromaleic acid (0.9 g, 5.9 mmol) and phosphorus pentoxide (1.3 g, 9 mmol) were carefully added under a nitrogen atmosphere and heated. The fraction distilling at 128°C afforded pure difluoromaleic

anhydride (0.3 g, 40%, colorless liquid, bp 127-128°C, lit.[5] 128 °C). ^{19}F NMR (282.3 MHz, $CDCl_3$): δ -137.9 (s, 2F) ppm.

Synthesis of difluoromaleic-^{18}O acid

Difluoromaleic anhydride (50 mg, 0.4 mmol) was added at 0°C under N_2 to a 10-mL round-bottomed flask containing a solution of sodium hydroxide-^{18}O (35 mg, 0.8 mmol) in $H_2{}^{18}O$ (500 μL) and stirred. The progress of the reaction was monitored by ^{19}F NMR for the appearance of signal corresponding to mono-^{18}O-labelled difluoromaleate dianion (-140.8 ppm, lit.[6] -140.1 ppm). The reaction was complete in 30 min, whereupon the reaction mixture was acidified with hydrochloric acid (1*N*, 1 mL) and evaporated to dryness on a rotary evaporator. The solid material thus obtained was sonicated in acetone (10 mL) for 1 min, filtered, and washed with acetone (2 x 10 mL), and the undissolved residue was discarded. The acetone extracts were combined and dried with anhydrous Na_2SO_4. The solvent was evaporated to dryness and the resulting solid was recrystallized from CH_2Cl_2 to afford difluoromaleic-^{18}O acid along with small amounts of other isotopologues (50 mg, 88%) white solid, mp 219-220 °C, lit.[5] 219-220°C). ^{19}F NMR (282.3 MHz, D_2O): δ -126.3 (m, 2F) ppm. ESI-HRMS 152.9891, calculated for $C_4HF_2{}^{16}O_3{}^{18}O_1^-$ $[M–H]^-$: 152.9891.

Synthesis of Bu_4N^+ protium difluoromaleate-^{18}O (**2**-*h*-$^{18}O_n$, n = 0,1,2) and of Bu_4N^+ deuterium difluoromaleate-^{18}O (**2**-*d*-$^{18}O_n$, n= 0,1,2)

Bu_4N^+ difluoromaleate-^{18}O (**2**-*h*-$^{18}O_n$; n = 0,1,2) was prepared by the addition of 1 equiv. of Bu_4N^+ CN^- to a solution of mono-^{18}O-labelled difluoromaleic acid in H_2O, followed by evaporation to dryness, without additional purification and without much change in the ratio of un-, mono-, and di- ^{18}O labeling of its precursor. Figure S2 shows the ^{1}H and ^{19}F NMR spectra of this material after solvent removal and dissolution in CD_3CN. The material was confirmed as the monoanion by comparison of the intensity of the ^{1}H signal at 20.33 ppm with the intensities of the n-butyl signals.

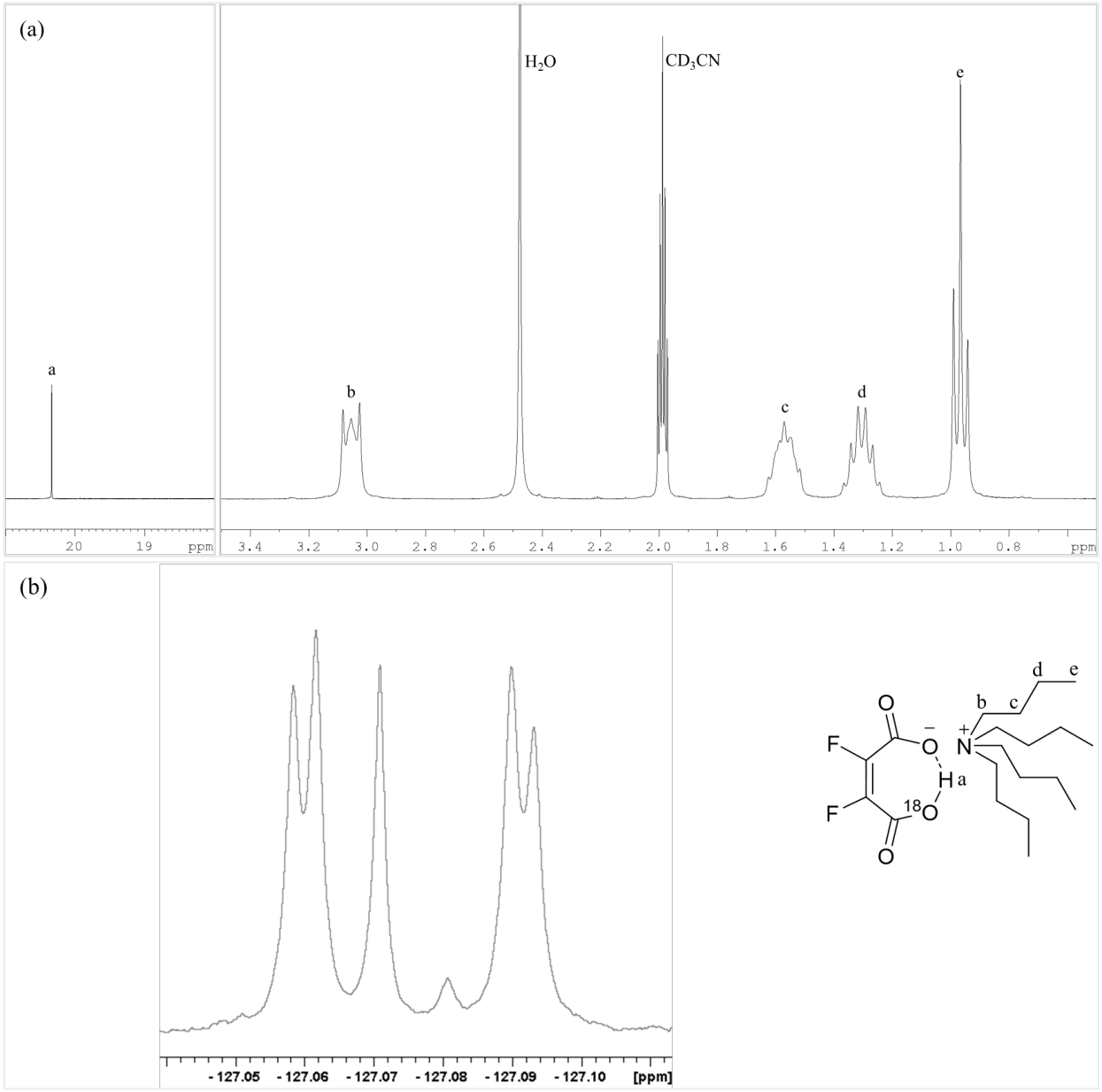

Figure S2. (a) ^{1}H NMR spectrum at 233.15 K and (b) ^{19}F NMR spectrum at room temperature of Bu_4N^+ protium difluoromaleate-^{18}O (**1**-*h*-$^{18}O_n$) in CD_3CN.

In a 2-mL vial ^{18}O-labeled difluoromaleic acid (10 mg, 66 μmol) was added and dissolved in water (500 μL) followed by addition of freshly prepared Bu_4N^+ CN^- solution in water (10 wt. %, 66 μmol, 172 μL). The mixture was stirred at room temperature for 5 min, and water and liberated HCN were removed under high vacuum, to obtain **2**-$^{18}O_n$ containing the mono-^{18}O-isotopologue as major product (25 mg, 99%, white solid). ^{1}H NMR (300 MHz) D_2O: δ 3.2 (m, 8H), 1.6 (m, 8H), 1.3 (m, 8H), 0.9 (t, 12H, J = 7.2 Hz) ppm. CD_3CN: δ 20.1 (s, 1H), 3.1

(m, 8H), 1.6 (m, 8H), 1.4 (m, 8H), 1.0 (t, 12H, J = 7.2 Hz) ppm. ^{19}F NMR (282.3 MHz) in D_2O: δ -126.4 (ABq, J = 2.6 Hz, 2F) ppm and in CD_3CN: δ -127.1 (ABq, J = 0.9 Hz, 2F) ppm. ESI-HRMS: 152.9891, calc. $C_4HF_2{}^{16}O_3{}^{18}O_1^-$ $[M–H]^-$: 152.9891.

In contrast to the above procedure the attempted synthesis of Bu_4N^+ deuterium difluoromaleate-^{18}O (**2**-*d*-$^{18}O_n$; n = 0,1,2) by the addition of 1 equiv. of Bu_4N^+ $CN^–$ to a solution of mono-^{18}O-labelled difluoromaleic acid in D_2O was not successful. We surmise that this is because difluoromaleic acid in aqueous solution is present exclusively as its monoanion, which is too weak an acid and also too weak a base that neither base- nor acid-catalyzed proton exchange is fast enough to equilibrate the protonated and deuterated isotopologues. To establish the equilibrium, which favors the deuterated form, it was necessary to heat in D_2O. Therefore ^{18}O-labeled-difluoromaleic acid (10 mg, 66 μmol) was dissolved in D_2O (500 μL) in a 2-mL vial and stirred at 95°C under N_2 for 20 min. A freshly prepared solution of Bu_4N^+ $CN^–$in D_2O (10 wt. %, 66 μmol, 175 μL) was then added to the reaction mixture, stirred at 95°C for 1 min, and quickly cooled to 0°C in an ice bath. Water and liberated HCN were removed under high vacuum to obtain **2**-*d*-$^{18}O_n$ containing the mono-^{18}O-isotopologue as major product (25 mg, 99%, white solid). Incorporation of deuterium in the product was > 99% and was confirmed by complete disappearance of the singlet at ~20 ppm in the ^{1}H NMR recorded in CD_3CN at 233 K. ^{1}H NMR (300 MHz) D_2O: δ 3.2 (m, 8H), 1.6 (m, 8H), 1.3 (m, 8H), 0.9 (t, 12H, J = 7.2 Hz) ppm. CD_3CN: δ 3.1 (m, 8H), 1.6 (m, 8H), 1.4 (m, 8H), 1.0 (t, 12H, J = 7.2 Hz) ppm. ^{19}F NMR (282.3 MHz) in D_2O: δ -126.3 (ABq, 2F, J = 2.7 Hz) ppm and, in CD_3CN: -127.0 (ABq, 2F, J = 1.5 Hz) ppm. Figure S3a shows the ^{1}H NMR spectrum at -40°C of this material after solvent removal and dissolution in CD_3CN. Figure S3b shows its ^{19}F NMR spectrum in CD_3CN at room temperature.

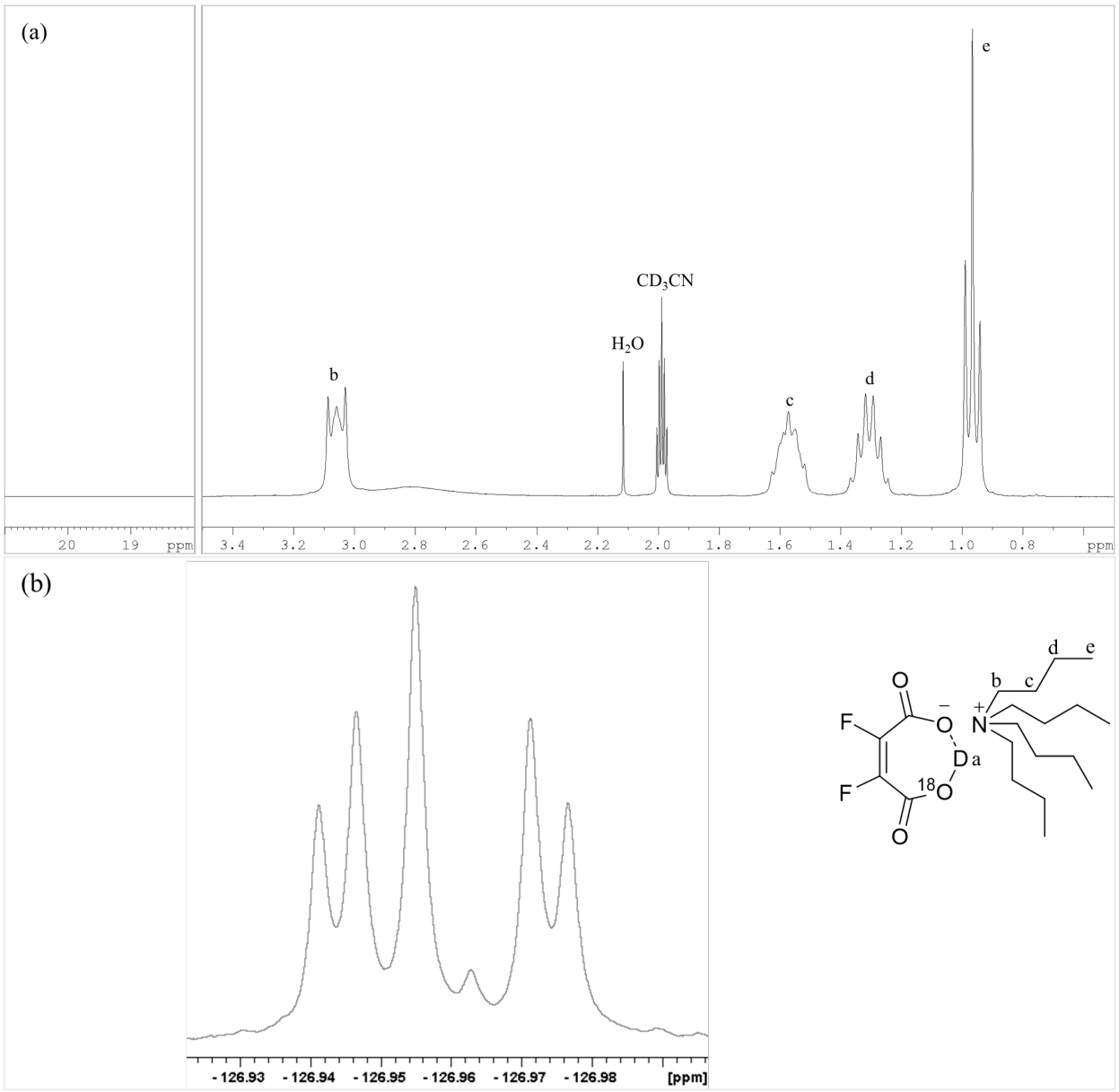

Figure S3. (a) ^{1}H NMR spectrum at 233.15 K and (b) ^{19}F NMR spectrum at room temperature of Bu_4N^+ deuterium difluoromaleate-^{18}O (**1**-*d*-$^{18}O_n$) in CD_3CN.

Analysis of Relative Amounts of ^{18}O-Isotopologues in **2**-*h*/*d*

Negative-ion ESI mass spectrometry of ^{18}O-labeled difluoromaleic acid ($[M–H]^-$ = 153 m/z for $C_4HF_2O_3{}^{18}O_1^-$) was used to measure $P(n)$ (n = 0,1,2), the fraction of the resulting ion **2** that is un-, mono-, or di-labeled. Values are presented in Table S4. Although different preparations produced slightly different ratios, they were all very similar, and Table S4 is representative.

Table S4. Masses and relative amounts of ^{18}O isotopologues in ^{18}O-labeled difluoromaleic acid.

Mass (*m/z*)	$n(^{18}O)$	$P(n)$
150.99	0	0.154
152.99	1	0.793
154.99	2	0.053

Variable-Temperature NMR Studies

The variable-temperature ^{19}F NMR spectra were obtained for samples prepared as 25-mM solutions of **2**-$^{18}O_n$ or **2**-*d*-$^{18}O_n$ in D_2O (273.15 – 313.15 K) or CD_3CN (233.15 – 313.15 K). The temperature in the NMR probe was calibrated with 4% CH_3OH in CD_3OD for 220-300 K and 80% ethylene glycol in DMSO-d_6 for 300-320 K according to standard procedure.[7] The room-temperature NMR spectra were recorded at 20°C. For every temperature, the probe was set to the desired temperature and allowed to equilibrate for 10-15 minutes, locked on D_2O or CD_3CN, tuned, and shimmed before the spectrum was acquired. The ^1H NMR spectra were obtained with sixteen transients, and a spectral window of 9.0 kHz (+25 to -5 ppm) was used, to include any deshielded OHO signal, with 16K data points zero-filled to a final resolution of 64 points/Hz. The ^{19}F NMR spectra were obtained with sixteen transients, and a spectral window of 1.4 kHz (-124 to -129 ppm) was used, with 32K data points zero-filled to 128 points/Hz. Enhancement of resolution was achieved by applying line broadening of only 0.1 Hz followed by exponential multiplication prior to Fourier transformation. Additionally, phase and baseline were corrected for any observed distortion on the spectra.

Analysis of ^{19}F NMR AB pattern

When two magnetically inequivalent nuclei are strongly coupled to each other ($\nu_0\Delta\delta \sim J$), an AB pattern is observed in the NMR spectrum, and second-order analysis is required.[8] The AB patterns observed in the ^{19}F spectra of monolabeled **2**-^{18}O and **2**-*d*-^{18}O are the outer signals in Fig. 5, with chemical shifts δ_1, δ_2, δ_3, and δ_4, from most shielded to least (from right to left). The coupling constant J_{AB} is given by eq S1, where ν_0 is the spectrometer frequency, 282 MHz. The chemical-shift difference between the two inequivalent ^{19}F, $\Delta\nu_{AB}$, is given by eq. S2. The intrinsic isotope shift, Δ_0, is given by half the difference between the chemical shifts of the two

central signals or, more accurately, by the difference between the chemical shift of **2**-$^{18}O_0$ and the average of δ_1, δ_2, δ_3, and δ_4, as in eq S3.

$$J = 10^{-6}\nu_0(\delta_1 - \delta_2) = 10^{-6}\nu_0(\delta_3 - \delta_4) \quad \text{(S1)}$$

$$\Delta\nu_{AB} = [(\delta_1 - \delta_4)(\delta_2 - \delta_3)]^{1/2} \quad \text{(S2)}$$

$$\Delta_0 = \delta_{18O0} - (\delta_1 + \delta_2 + \delta_3 + \delta_4)/4 \quad \text{(S3)}$$

Chemical-Shift Differences Between 1-*h* and 1-*d* and Between 2-*h* and 2-*d*

Tables S5 and S6 list the chemical shifts for the carboxyl (**A**) and ipso (**B**) carbons for ^{18}O isotopologues of **1**-*h* and **1**-*d*, respectively, at various temperatures. They are arranged in order of increasing shielding. Although the values are listed to four places after the decimal, ten places were retained for all calculations. The values in Table S5 differ insignificantly from those previously reported,[9] but these are most comparable to the ones in Table S6.

Table S5. ^{13}C Chemical shifts (ppm) for carboxyl (**A**) and ipso (**B**) carbons of ^{18}O isotopologues of **1**-*h* at various temperatures.

Peak	20°C	−10°C	−20°C	−30°C	−50°C
$\mathbf{A_0}$	171.3578	171.5141	171.5624	171.6206	171.7167
$\mathbf{A_1}$	171.3267	171.4813	171.5294	171.5867	171.6827
$\mathbf{B_{01}}$	139.3524	139.4090	139.4337	139.4596	139.5068
$\mathbf{B_{00/11}}$	139.3291	139.3836	139.4074	139.4328	139.4801
$\mathbf{B_{10}}$	139.3064	139.3578	139.3815	139.4061	139.4516

Table S6. ^{13}C Chemical shifts (ppm) for carboxyl (**A**) and ipso (**B**) carbons of ^{18}O isotopologues of **1**-*d* at various temperatures.

Peak	20°C	−10°C	−20°C	−30°C	−50°C
$\mathbf{A_0}$	171.3631	171.4655	171.5028	171.5527	171.6597
$\mathbf{A_1}$	171.3346	171.4323	171.4681	171.5178	171.6239
$\mathbf{B_{01}}$	139.2853	139.3458	139.3637	139.3846	139.4320
$\mathbf{B_{00/11}}$	139.2573	139.3157	139.3329	139.3525	139.3974
$\mathbf{B_{10}}$	139.2297	139.2858	139.3022	139.3204	139.3622

At 20°C the carboxyl chemical-shift separation for **1**-*d* in Table S6 is smaller than for **1**-*h* in Table S5, which would suggest a symmetric H-bond. However, the signal for $\mathbf{A_1}$ at 20°C is splitting into two peaks, so this chemical shift is less reliable. In contrast, at −10°C, −20°C, −30°C, and −50°C the chemical-shift separations for **1**-*d* are larger than for **1**-*h*. Because of this disagreement, and because all these separations are small, it is more reliable to focus on chemical-shift separations at ipso carbons (**B**).

To convert the temperature dependences in Tables 1 and 2 to $\Delta\Delta G°$, the ^{18}O isotope effect on the free energy, and K_{16}/K_{18}, the equilibrium isotope effect, equations S4 and S5 were used, where Δ is the observed chemical-shift difference, Δ_0 is the intrinsic difference, D is the chemical-shift separation between diacid and dianion (6 ppm in ^{13}C NMR of **1** or 29 ppm in ^{19}F NMR of **2**), as estimated by doubling the chemical-shift separation between the diacid and the monoanion, and R is the gas constant.

$$\Delta = \Delta_0 - \frac{D}{2}\frac{\Delta\Delta G^o}{RT} \quad \text{(S4)}$$

$$\Delta\Delta G^o = -RT\ln K \quad \text{(S5)}$$

The variable-temperature ^{19}F NMR chemical shifts of **2**-*h*-$^{18}O_n$ and **2**-*d*-$^{18}O_n$ in Fig. 6 are collected in Tables S7 and S8. Although the values are all negative, they too are arranged in order of increasing shielding. Also, although the values are listed to four places after the decimal, ten places were retained for all calculations.

Table S7. Temperature-dependence of ^{19}F NMR chemical shifts (ppm) of **2**-*h*-$^{18}O_n$ in D_2O.

T,ºC	δ_1	δ_2	$\delta^{18}O_0$	$\delta^{18}O_2$	δ_3	δ_4
0	-126.4184	-126.4282	-126.4461	-126.4520	-126.4708	-126.4805
10	-126.4190	-126.4285	-126.4463	-126.4516	-126.4698	-126.4793
20	-126.4195	-126.4288	-126.4462	-126.4512	-126.4691	-126.4784
30	-126.4202	-126.4293	-126.4462	-126.4511	-126.4686	-126.4777
40	-126.4204	-126.4294	-126.4462	-126.4498	-126.4676	-126.4766

Table S8. Temperature-dependence of ^{19}F NMR chemical shifts (ppm) of **2**-*d*-$^{18}O_n$ in D_2O.

T,ºC	δ_1	δ_2	$\delta^{18}O_0$	$\delta^{18}O_2$	δ_3	δ_4
0	-126.3061	-126.3161	-126.3330	-126.3424	-126.3590	-126.3690

10	-126.3070	-126.3168	-126.3332	-126.3421	-126.3584	-126.3682
20	-126.3074	-126.3170	-126.3330	-126.3416	-126.3576	-126.3672
30	-126.3081	-126.3176	-126.3332	-126.3415	-126.3572	-126.3667
40	-126.3086	-126.3180	-126.3331	-126.3414	-126.3566	-126.3660

Figures S2 and S3 show the ^{19}F NMR spectra of Bu_4N^+ protium and deuterium difluoromaleate-^{18}O (**1**-*h*-$^{18}O_n$ and **1**-*d*-$^{18}O_n$) in CD_3CN at 20ºC. Spectra at lower temperatures were poorly resolved and not useful. It is not clear why the apparent coupling constant J_{AB} is larger for the latter, opposite to the behavior in D_2O (Fig. 6 and Table 2).

Evidence for a Greater Anharmonicity with H than with D

According to elementary quantum mechanics, the mean square amplitude for the $n = 0$ level of a harmonic oscillator with force constant k and reduced mass μ is given in eq S6,[10] so that the amplitude for H motion, with its greater reduced mass, indeed ought to be larger than for D.

$$\langle x^2 \rangle = \frac{1}{2}\frac{h\nu}{k} = \frac{h}{4\pi}\frac{1}{\sqrt{k\mu}} \qquad \text{(S6)}$$

To take anharmonicity explicitly into account, time-averaged vibrational calculations were performed on Hmaleate (**S1**-*h*) and Dmaleate (**S1**-*d*) monoanions at the RMPW1PW91/6-311G(d,p) level,[11] comparable to the calculation level of Bogle and Singleton.[12] Table S9 lists the amplitudes of independent Cartesian coordinates for **S1**-*h* and **S1**-*d* at both 0 K and 298 K. It can be seen that there are only very small differences between **S1**-*h* and **S1**-*d* at most atoms, except that the amplitudes for H_{11} are significantly greater than for D_{11}, along all three directions. Again the amplitude for H motion is shown to be larger than for D.

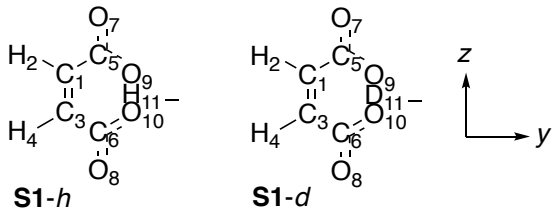

Table S9. Root-mean-square amplitudes (Å) of Cartesian coordinates for anharmonic motion of C1, H2, C5, O7, O9, and H11 or D11 in **S1**-*h* and **S1**-*d*.

coord	**S1**-*h*, 0K	**S1**-*d*, 0K	**S1**-*h*, 298K	**S1**-*d*, 298K
x_1	0.072	0.072	0.154	0.155
y_1	0.035	0.035	0.038	0.038
z_1	0.041	0.041	0.046	0.045
x_2	0.169	0.170	0.271	0.273
y_2	0.111	0.111	0.113	0.113
z_2	0.092	0.092	0.094	0.094
x_5	0.042	0.042	0.048	0.048
y_5	0.036	0.036	0.040	0.041
z_5	0.042	0.040	0.058	0.057
x_7	0.074	0.075	0.185	0.185
y_7	0.035	0.035	0.041	0.042
z_7	0.037	0.037	0.048	0.050
x_9	0.067	0.066	0.140	0.139
y_9	0.037	0.036	0.044	0.042
z_9	0.037	0.037	0.045	0.045
x_{11}	0.119	0.100	0.151	0.136
y_{11}	0.275	0.237	0.460	0.449
z_{11}	0.101	0.085	0.102	0.086

Table S10 provides a clearer comparison of the anharmonic motions. It shows the ratio of the total amplitude, $[\langle x^2\rangle+\langle y^2\rangle+\langle z^2\rangle]^{1/2}$, for motion in **S1**-*h* relative to **S1**-*d*, for each independent atom. The motions of distant C-H and carbonyl oxygens O7,8 are greater in **S1**-*d*, opposite to the expectation from eq S6, but very slightly. The motions of carboxyl carbons C5,6 and of H-bonded oxygens O9,10 are significantly greater in **S1**-*h*. The largest difference is in the anharmonic motions of the H relative to D, especially at 0 K, although the difference is reduced at 298 K because excited vibrational states are more extensively populated for D. Thus these computations document the assertion that anharmonicity is generally greater with H than with D. Therefore we would have expected that if the previously observed isotope shifts were due to the

anharmonicity of hydrogen motion in a symmetric H-bond, smaller isotope shifts should have been observed with D in the H-bond, contrary to our observations.

Table S10. Ratio of total amplitudes of Cartesian coordinates for anharmonic motion of independent atoms in **S1**-*h* relative to total ampitudes in **S1**-*d*.

atom	A_h/A_d, 0K	A_h/A_d, 298K
C1	0.999	0.996
H2	0.999	0.996
C5	1.014	1.002
O7	0.998	0.994
O9	1.006	1.009
H/D11	1.167	1.037

References

(1) Baeyer, A. Ueber die Constitution des Benzols. Fünfte Abhandlung. Ueber die Reductionsproducte der Phtalsäure. *Justus Liebigs Ann. Chem.* **1890**, *258*, 145-219.

(2) Okabe, A.; Fukushima, T.; Ariga, K.; Niki, M.; Aida, T. Tetrafluoroborate Salts as Site-Selective Promoters for Sol−Gel Synthesis of Mesoporous Silica. *J. Am. Chem. Soc.* **2004**, *126*, 9013-9016.

(3) Emsley, J. W.; Phillips, L. Fluorine Chemical Shifts. *Prog. Nucl. Magn. Reson. Spectrosc.* **1971**, *7*, 1-520.

(4) Perrin, C. L.; Thoburn, J. D. Symmetries of Hydrogen Bonds in Monoanions of Dicarboxylic Acids. *J. Am. Chem. Soc.* **1992**, *114*, 8559-8565.

(5) Raasch, M. S.; Miegel, R. E.; Castle, J. E. Mono- and Difluorobutenedioic Acids. *J. Am. Chem. Soc.* **1959**, *81*, 2678-2680.

(6) Perrin, C. L.; Karri, P.; Moore, C.; Rheingold, A. L. Hydrogen-Bond Symmetry in Difluoromaleate Monoanion. *J. Am. Chem. Soc.* **2012**, *134*, 7766-7772.

(7) Findeisen, M.; Brand, T.; Berger, S. A ^{1}H-NMR Thermometer Suitable for Cryoprobes. *Magn. Reson. Chem.* **2007**, *45*, 175-178.

(8) Becker, E. D. *High Resolution NMR: Theory and Chemical Applications*; Elsevier, 1999.

(9) Perrin, C. L.; Burke, K. D. Variable-Temperature Study of Hydrogen-Bond Symmetry in Cyclohexene-1,2-dicarboxylate Monoanion in Chloroform-*d*. *J. Am. Chem. Soc.* **2014**, *136*, 4355-4362.

(10) Levine, I. N. *Quantum Chemistry*; 2 ed.; Allyn and Bacon, 1974; p 374.

(11) M. J. Frisch, G. W. T., H. B. Schlegel, G. E. Scuseria, M. A. Robb, J. R. Cheeseman, G. Scalmani, V. Barone, B. Mennucci, G. A. Petersson, H. Nakatsuji, M. Caricato, X. Li, H. P. Hratchian, A. F. Izmaylov, J. Bloino, G. Zheng, J. L. Sonnenberg, M. Hada, M. Ehara, K. Toyota, R. Fukuda, J. Hasegawa, M. Ishida, T. Nakajima, Y. Honda, O. Kitao, H. Nakai, T. Vreven, J. A. Montgomery, Jr., J. E. Peralta, F. Ogliaro, M. Bearpark, J. J. Heyd, E. Brothers, K. N. Kudin, V. N. Staroverov, T. Keith, R. Kobayashi, J. Normand, K. Raghavachari, A. Rendell, J. C. Burant, S. S. Iyengar, J. Tomasi, M. Cossi, N. Rega, J. M. Millam, M. Klene, J. E. Knox, J. B. Cross, V. Bakken, C. Adamo, J. Jaramillo, R. Gomperts, R. E. Stratmann, O. Yazyev, A. J. Austin, R. Cammi, C. Pomelli, J. W. Ochterski, R. L. Martin, K. Morokuma, V. G. Zakrzewski, G. A. Voth, P. Salvador, J. J. Dannenberg, S. Dapprich, A. D. Daniels, O. Farkas, J. B. Foresman, J. V. Ortiz, J. Cioslowski, and D. J. Fox. Gaussian, Inc., Wallingford, CT, 2013.

(12) Bogle, X. S.; Singleton, D. A. Isotope-Induced Desymmetrization Can Mimic Isotopic Perturbation of Equilibria. On the Symmetry of Bromonium Ions and Hydrogen Bonds. *J. Am. Chem. Soc.* **2011**, *133*, 17172-17175.